



TECHNICAL PAPER

Further Investigations Into the Interactions Between Cinema Loudspeakers and Screens

By Brian Long, Roger Schwenke, Peter Soper, and Glenn Leembruggen

Modern-day data-acquisition techniques allow the gathering of high-resolution polar data to assess the detailed performance of loudspeakers. While these techniques are now common in engineering laboratories, they can also be used for acoustic investigation into the in situ performance of loudspeakers. This paper uses modern high-resolution data-acquisition techniques and analysis tools to investigate the complexity of the interaction between a loudspeaker and the screen in a cinema presentation environment. A discussion is presented that explores the effects of three types of screen materials on loudspeaker frequency responses and radiation patterns. These screen effects are explored using a range of loudspeaker-screen distances found in typical cinemas. The impact of the screen on patron listening experience is examined, particularly in relation to the standards for system response set out in SMPTE Timed Text 202:2010.

INTRODUCTION

Since the first “talkie” and use of reproduced sound in motion pictures, much work has been done to advance the performance of cinema audio systems. This work has focused on the evolution of loudspeaker technology and signal processing and the refinement of the cinema acoustical environment. However, the effect of one important component in the playback chain has received little attention: the screen. In their 1985 paper regarding the upgrade of the sound system for the Academy of Motion Picture Arts and Sciences, Eargle, Bonner, and Ross noted that “the effect of perforated vinyl motion picture screens on sound transmission is not well understood” and mentioned that observed losses were likely due to reflections from the screen.¹

Although advances have been made in screen material technology and perforation styles, they have been more of an afterthought when compared to improvements in audio hardware. Since 1985, only slight mention of the importance of the interaction of loudspeakers and screens has been made. In 1990, Allen, Hunter, Geist, and Delgado investigated screen interactions with loudspeakers and introduced concepts such as “beam spreading” to support the case for four-way speakers over two-way speakers.² This study tested the effect of inserting a screen between the loudspeaker and the listening area.

In 1997, when the academy renovated its sound system, further work was undertaken by Eargle et al. that went beyond the work of Allen et al. and provided data with a screen at different distances from the loudspeakers. In the mid-2000s, the authors began a study of the factors that degraded performance in cinema systems. As part of this program, high-resolution data-acquisition techniques were utilized to conduct measurements in an anechoic space that would examine the effects of screens and the concept of beam spreading at a finer resolution than was previously possible.

The current study compares screens commonly used in commercial cinema and post-production facilities. Screens compared were the theater-perforated (theater-perf) screen, with a perforation diameter of approximately 1.2mm and a perforation ratio of 4.5%; the mini-perforated (mini-perf) screen, with a hole diameter of approximately 0.5mm and a perforation ratio of 1.7%; and the woven fabric screen.

Two approaches were used to explore the issue of screen interactions from both practical and theoretical perspectives:

- Measurement of the changes that a screen makes to the loudspeaker's response over a range of angles. These measurements directly show the impact of the screen over the listening area and on the loudspeaker's radiation pattern. Each of these screens was placed 150mm (6 in.), 300mm (12 in.), and 450mm (18 in.) from a loudspeaker in an anechoic space and measured at various incidence angles commensurate with in situ positioning in a cinema.
- Measurement of the normal-incidence acoustic properties of the screen using a plane-wave tube. The reflection and transmission factors of each screen type were established using measurements in the tube, with the incident sound striking the screen at an angle of 90° to the screen sample. These data can be directly related to the field use, where loudspeaker sound strikes the screen at 90°.

LOUDSPEAKER MEASUREMENTS

Overview

High-resolution polar data of the loudspeaker and screen behavior were captured in both horizontal and vertical planes. These mea-



Figure 1. Speaker and screen with the positioning apparatus used in the anechoic chamber.

sured data were stored in a database to allow a client to access the data via a network or Internet, create graphical representations of the data, and make predictions about interactions of multiple data sets at points within a two-dimensional plane.

Polar Scan Setup

The screen samples were fixed to the positioner in the anechoic chamber as shown in **Fig. 1**, with the desired angle between the screen and the loudspeaker, a two-way unit with a 100mm (4 in.) compression driver and 300mm (15 in.) low-frequency driver. A scan was then performed by rotating the apparatus through 360° in the plane being measured (horizontal or vertical) at 1° increments with 1/48th octave resolution from a microphone in the listening

area, in conformance with the Audio Engineering Society standard AES-5id. This measurement apparatus and the multipurpose acoustical prediction program (MAPP Online) for displaying the data are described in the literature.³⁻⁵ A library with a variety of loudspeaker and screen measurement data is available to interact free of charge via Meyer Sound's MAPP Online Pro Cinema acoustical prediction program.⁶

High-Resolution Polar Data

Initially, the polar pattern of a linear two-way loudspeaker with a nominal 80° horizontal and 50° vertical pattern was measured in an anechoic chamber without any screen obstruction in front of the loudspeaker. Next, the three screen types were introduced, and the measurements were repeated. The measurement data were then imported into the MAPP software for visualization and analysis.

Microphones were placed within the software analysis tool at the following positions:

- Microphone 1—on the axis of the loudspeaker at a distance of 6.1 m (20 ft).
- Microphone 2—in the horizontal plane, 40° off axis at the edge of the manufacturer-specified coverage pattern at a distance of 6.1 m (20 ft) from the loudspeaker; in the vertical plane, 25° off axis at the edge of the manufacturer's specified coverage.
- Microphone 3—in the horizontal plane, 140° off axis 3 m (10 ft) behind the acoustic center of the loudspeaker, which is 180° away from the microphone 2 position; in the vertical plane, 155° off axis and 180° away from microphone 2.

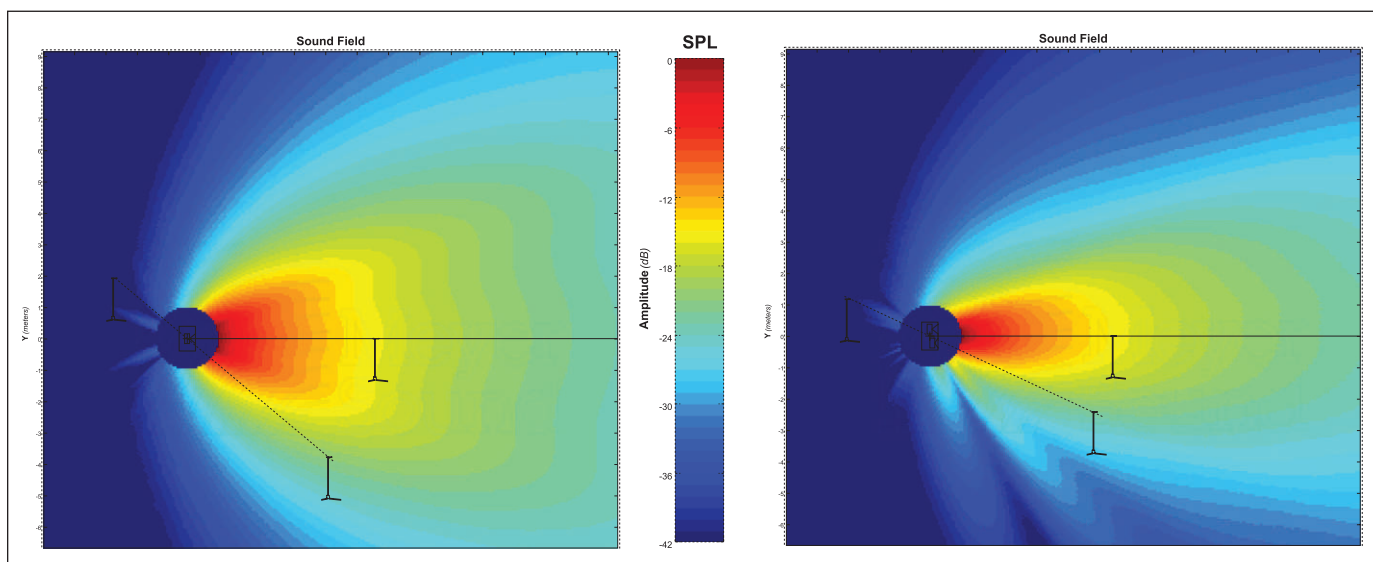


Figure 2. SPL distribution in the horizontal plane at 4 kHz without a screen.

Figure 3. SPL distribution in the vertical plane at 4 kHz without a screen.

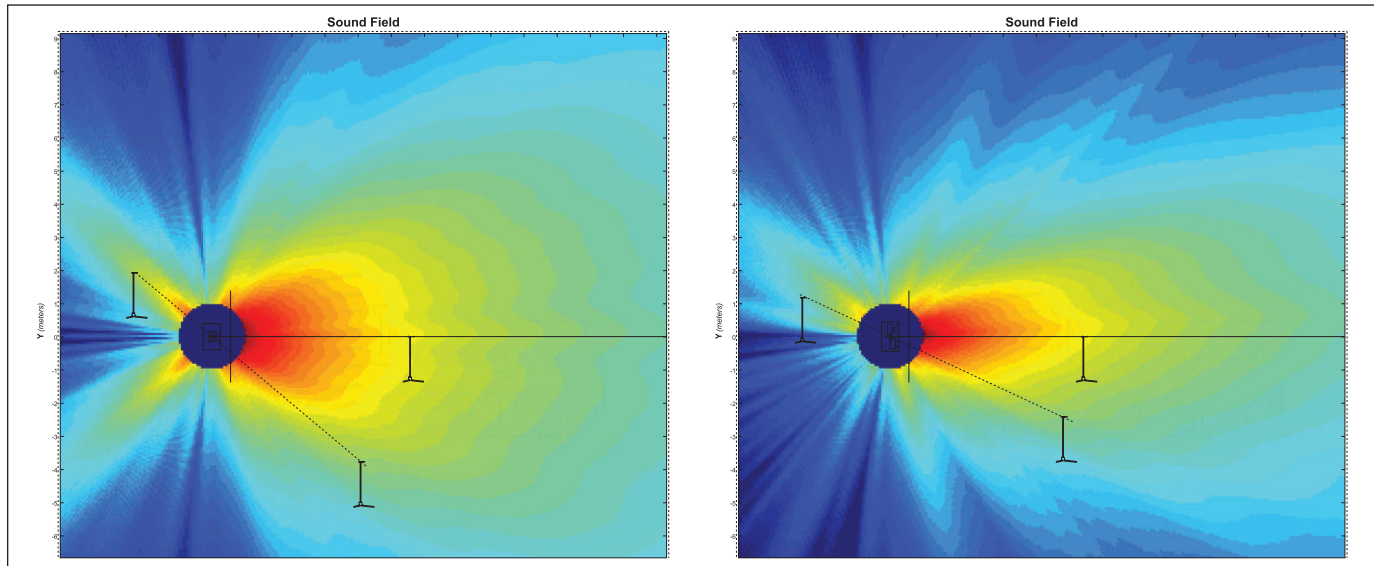


Figure 4. Sound pressure plots centered on a frequency of 4 kHz with a theater-perf screen 300mm (12 in.) from the loudspeaker.

Figures 2 and 3 show the loudspeaker's measured radiation patterns at 4 kHz in the horizontal and vertical planes. **Figures 4-6** show how the loudspeaker's radiation pattern changes with the introduction of different types of screens at a fixed distance of 300mm (12 in.).

Results from the three receiver microphones in the horizontal plane are shown in **Figs. 7-22**.

As earlier papers have shown, screens appear to produce an increase in sound levels beyond the normal coverage pattern of the speaker. This effect was hypothesized to be "screen spreading" akin to a Fresnel lens. However, the change in level is not monotonic with angle, with the largest increase in off-axis energy occurring behind the screen. This result becomes evident when comparing **Figs. 2 and 3** with **Figs. 4 and 5**.

The impulse response (IR) measured at the edge of the loudspeaker's horizontal radiation pattern without a screen is shown in **Fig. 7**. **Figures 8 and 9** show the IR at the same location with the theater-perf and mini-perf screens in place. It can be seen that the presence of those screens introduces a series of distinct late arrivals into the IR. Compared to the IRs of the perforated screens, the woven screen IR of **Fig. 10** is most similar to the no-screen case.

The multiple late arrivals in the IRs are due to successive reflections between the screen and the loudspeaker, which are somewhat analogous to a flutter echo. However, the irregular profile of the baffle and the diffraction effects of the horn and baffle edges produce some scattering during successive reflections, and because IR is presented on a linear scale, their levels are visually suppressed.

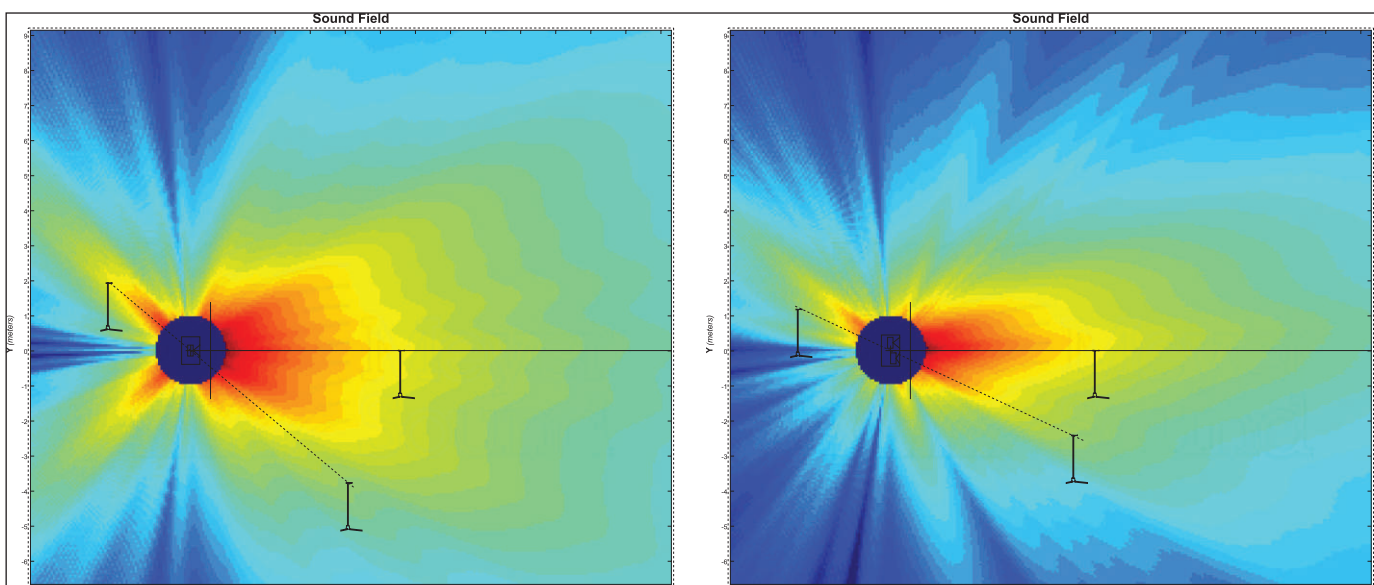


Figure 5. Sound pressure plots centered on a frequency of 4 kHz with a mini-perf-style screen 300mm (12 in.) from the loudspeaker.

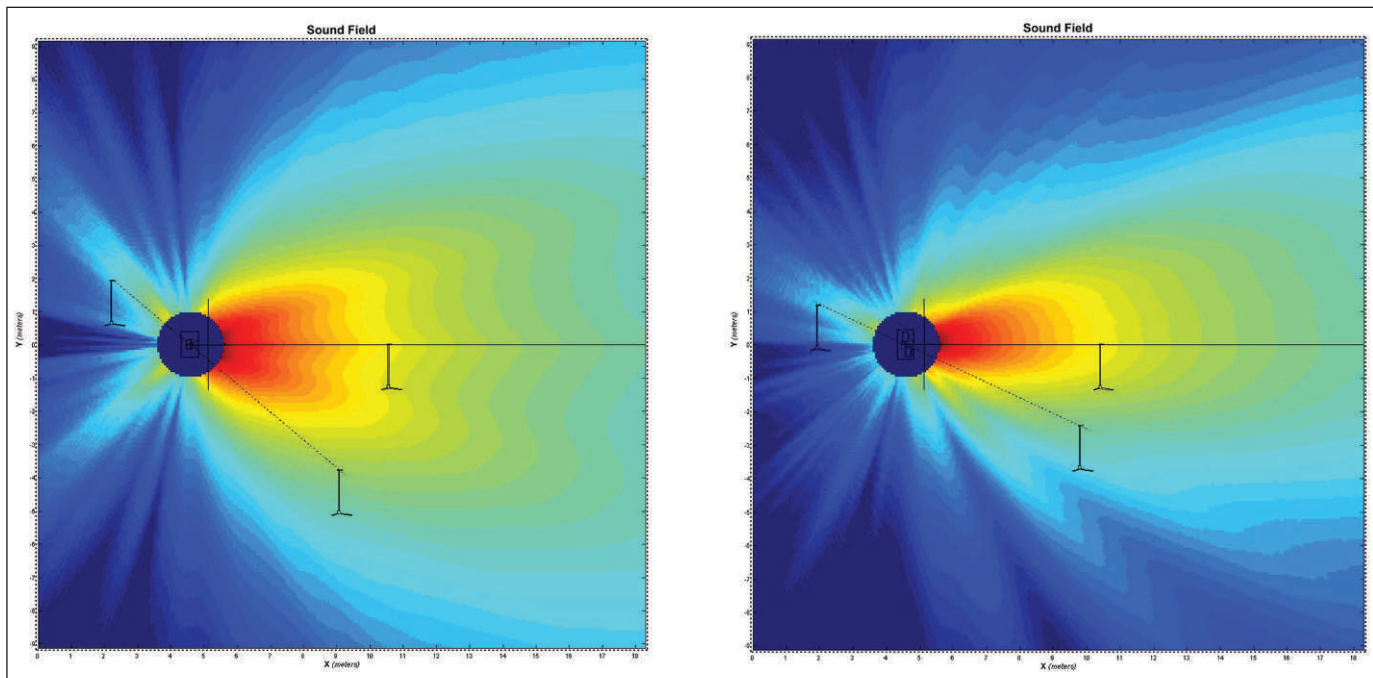


Figure 6. Sound pressure plots centered on a frequency of 4 kHz with a woven screen 300mm (12 in.) from the loudspeaker.

The effect of these late arrivals is seen in the unsmoothed frequency response graphs in **Figs. 11-13**, which compare the frequency responses of the four screen types at three positions with the loudspeaker-screen distance held constant. These high-resolution measurements show narrowband interactions that mostly affect frequencies above 2 kHz; however, changes are noticeable as low as 500 Hz. Overall, there is significant degradation of the loudspeaker frequency responses by the reflected energy from the screen.

These high-resolution impulse and frequency responses show that these changes in the sound levels at the edges of the horizontal pattern are due not to screen spreading of the loudspeaker's direct sound but rather to constructive and destructive interference between the direct sound and the sound reflected between the screen and the loudspeaker.

In addition, there is significant sound traveling backward from the screen, as can be seen in the frequency responses for the microphone 3 position (140°) in **Fig. 13**. This figure should be viewed in conjunction with the spatial distributions of sound shown in **Figs. 4-6**. Reflections from the screen can be regarded as emanating from an image source of the loudspeaker located in front of the screen (without the screen present). Because this image source has the same polar pattern as the loudspeaker, microphone 3 represents the edge of the horizontal pattern of this image source. The polar pattern of the image source is obstructed by the loudspeaker cabinet, which results in the null directly behind the loudspeaker in **Figs. 4-6**.

Figures 14-17 show measured responses at varying angles of incidence to the screen from the loudspeaker axis for each screen type.

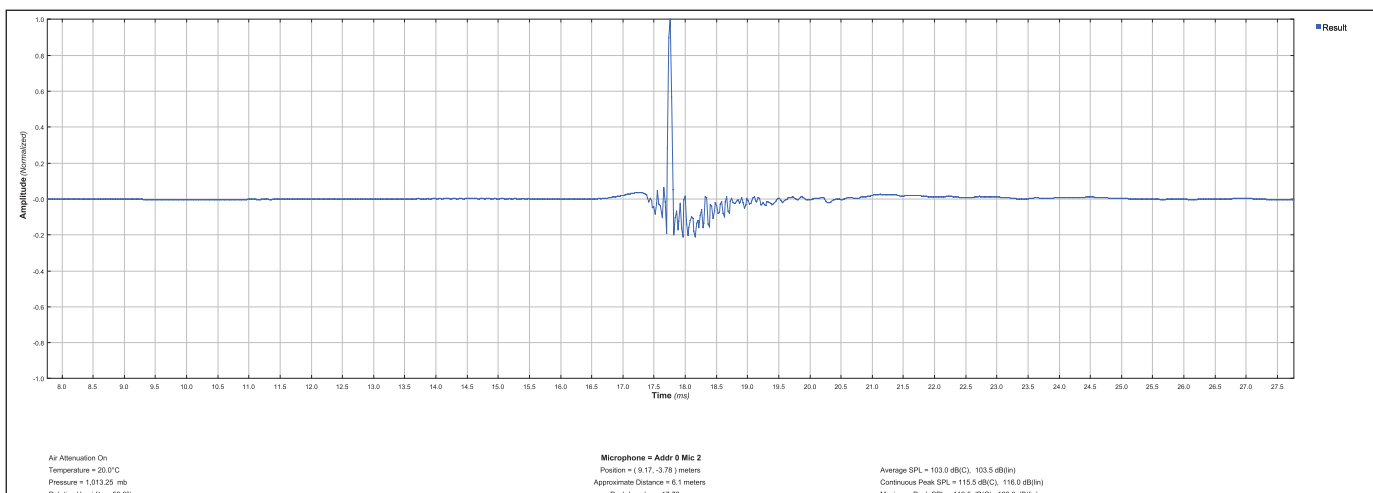


Figure 7. IR at microphone 2 and 40° off the horizontal loudspeaker axis without a screen.



FURTHER INVESTIGATIONS INTO THE INTERACTIONS BETWEEN CINEMA LOUDSPEAKERS AND SCREENS continued

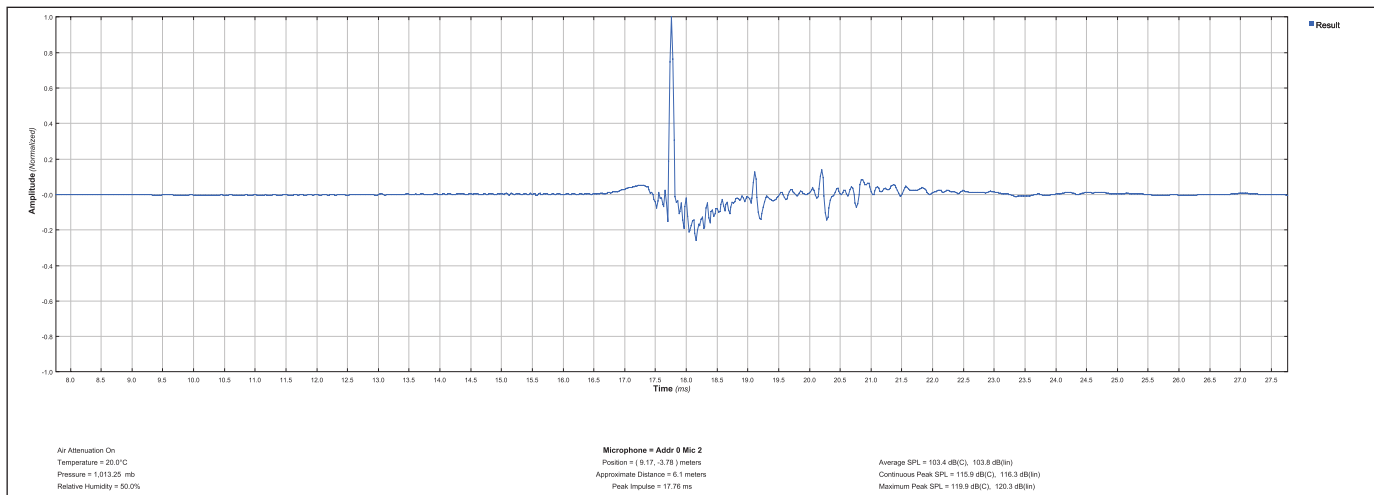


Figure 8. IR at microphone 2 and 40° off the horizontal loudspeaker axis with a theater-perf screen 300mm (12 in.) from the loudspeaker.

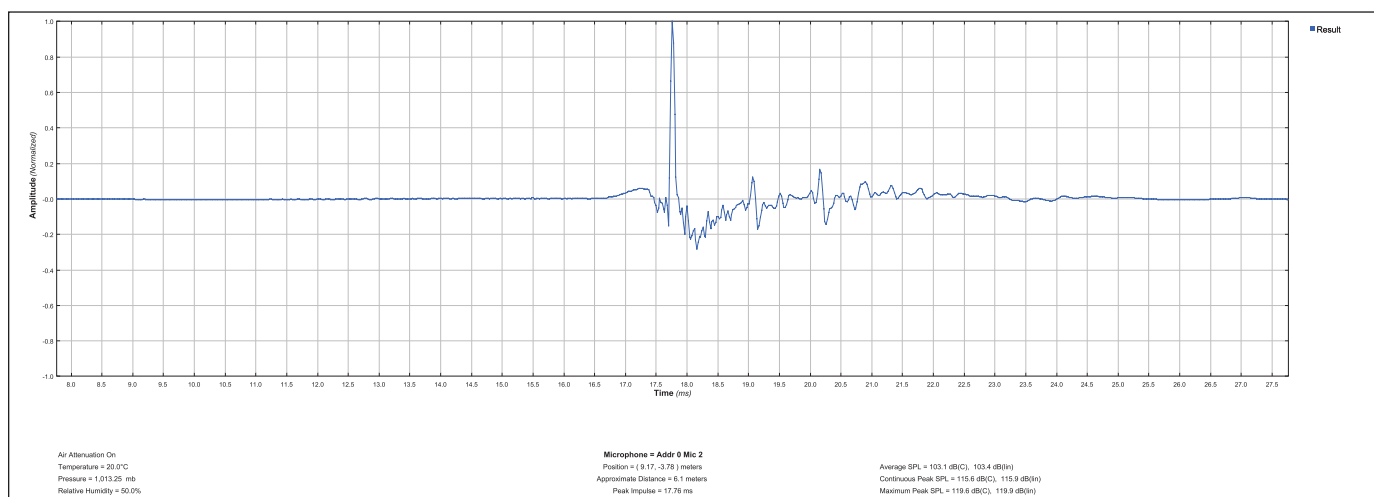


Figure 9. IR at microphone 2 and 40° off the horizontal loudspeaker axis with a mini-perf screen 300mm (12 in.) from the loudspeaker.

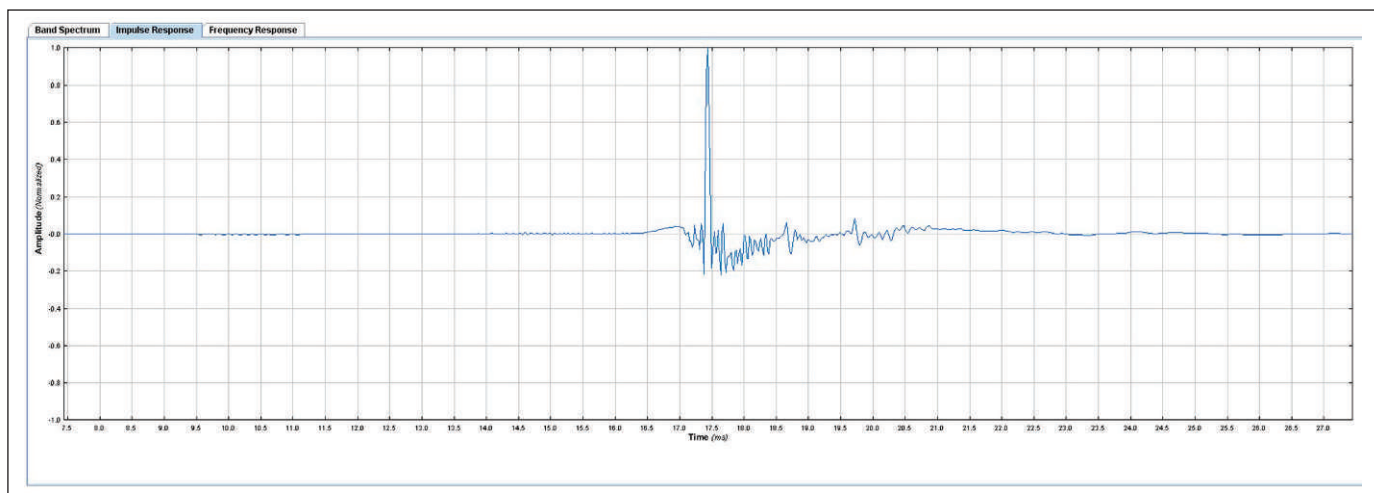


Figure 10. IR at microphone 2 and 40° off the horizontal loudspeaker axis with a woven screen 300mm (12 in.) from the loudspeaker.

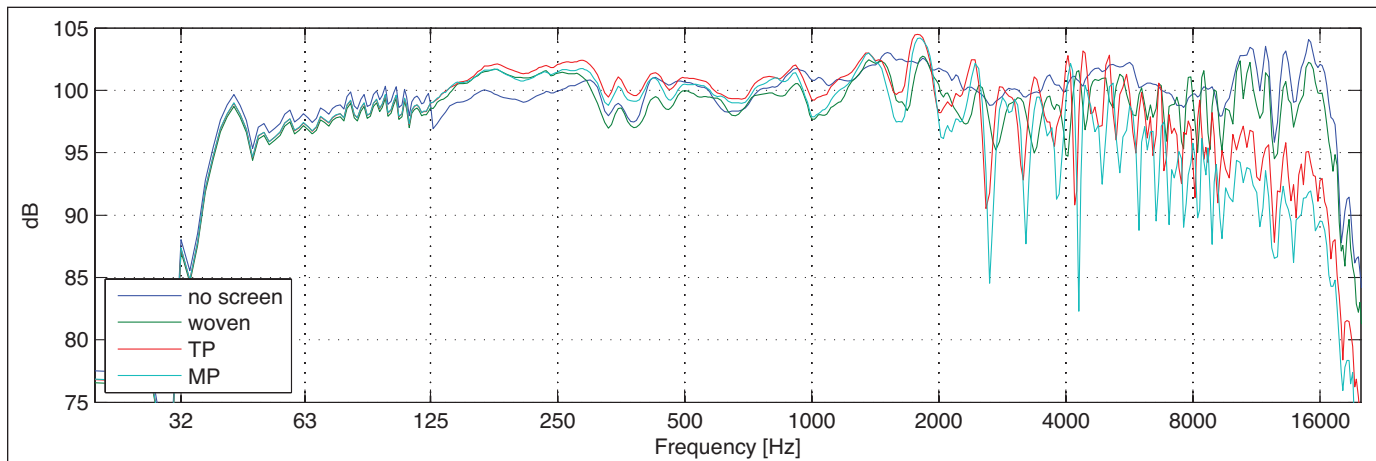


Figure 11. Effect of screen type on the axis of the loudspeaker at 300 mm (12 in.) TP = theater-perf, MP = mini-perf.

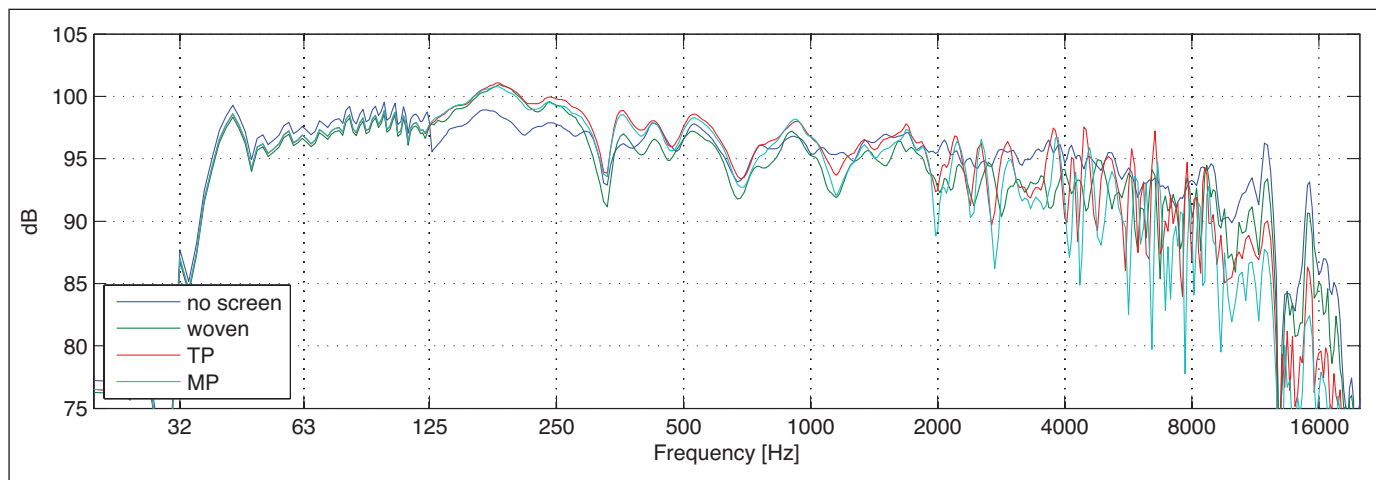


Figure 12. Effect of screen type 40° off the loudspeaker axis. TP = theater-perf, MP = mini-perf.

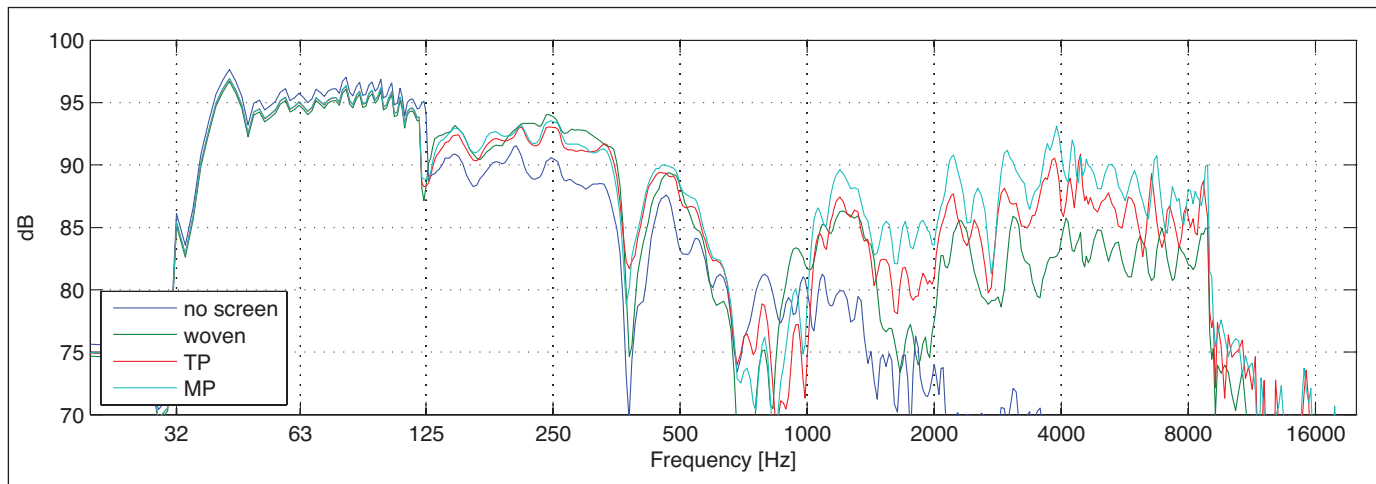


Figure 13. Effect of screen type 140° off the loudspeaker axis. TP = theater-perf, MP = mini-perf.



FURTHER INVESTIGATIONS INTO THE INTERACTIONS BETWEEN CINEMA LOUDSPEAKERS AND SCREENS continued

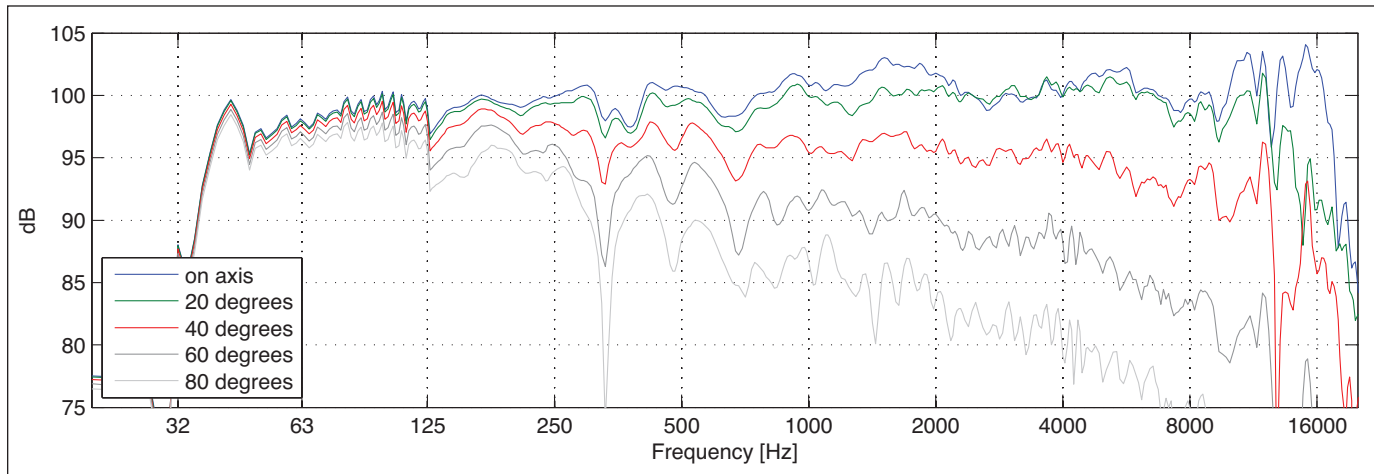


Figure 14. Responses at different angles with the loudspeaker without a screen.

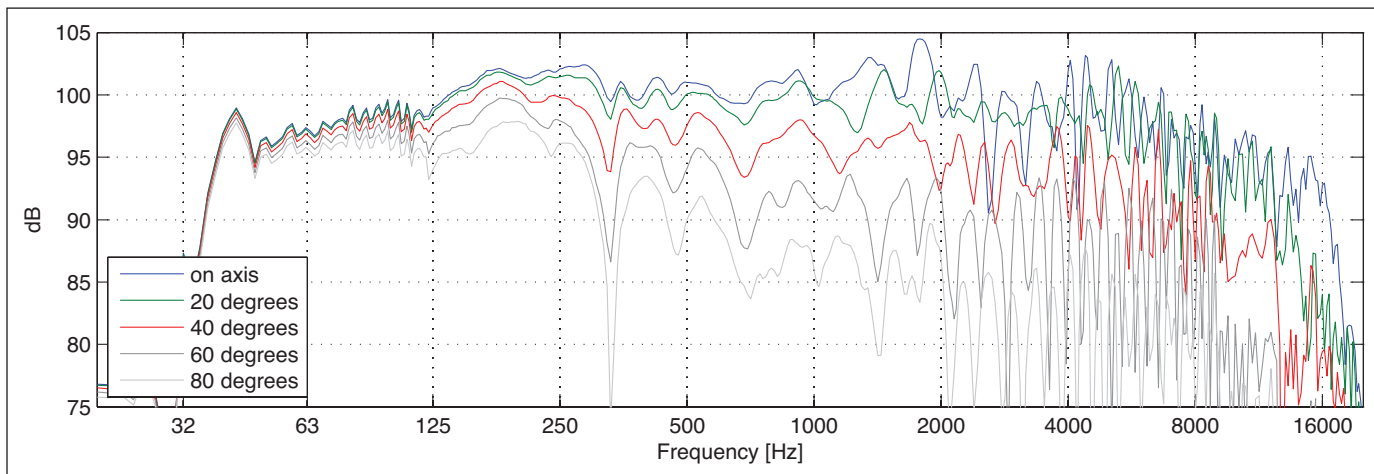


Figure 15. Responses at different angles with the loudspeaker 300mm (12 in.) from a theater-perf screen.

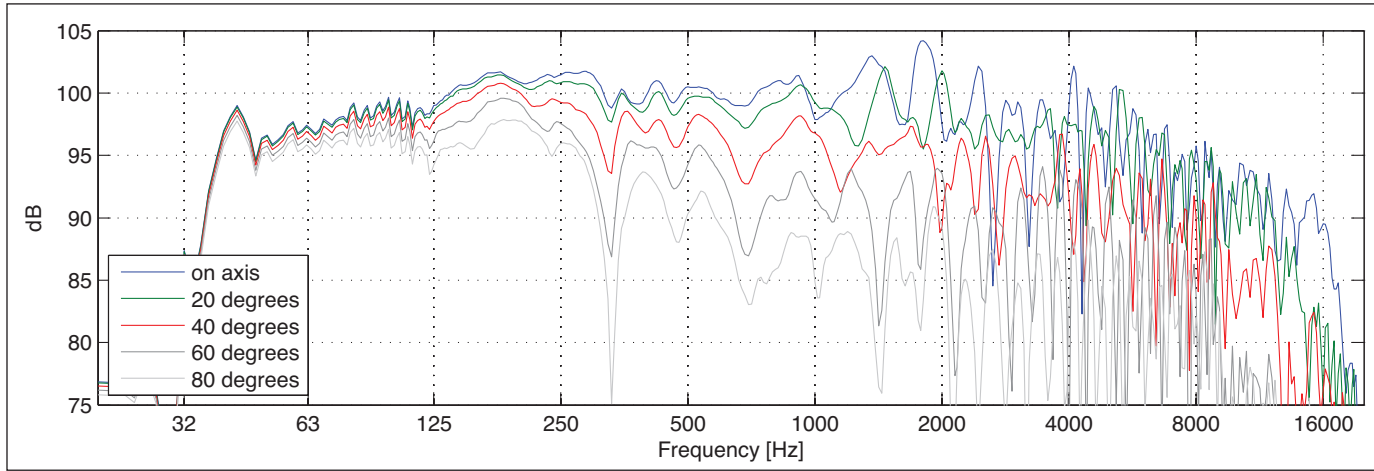


Figure 16. Responses at different angles with the loudspeaker 300mm (12 in.) from a mini-perf screen.

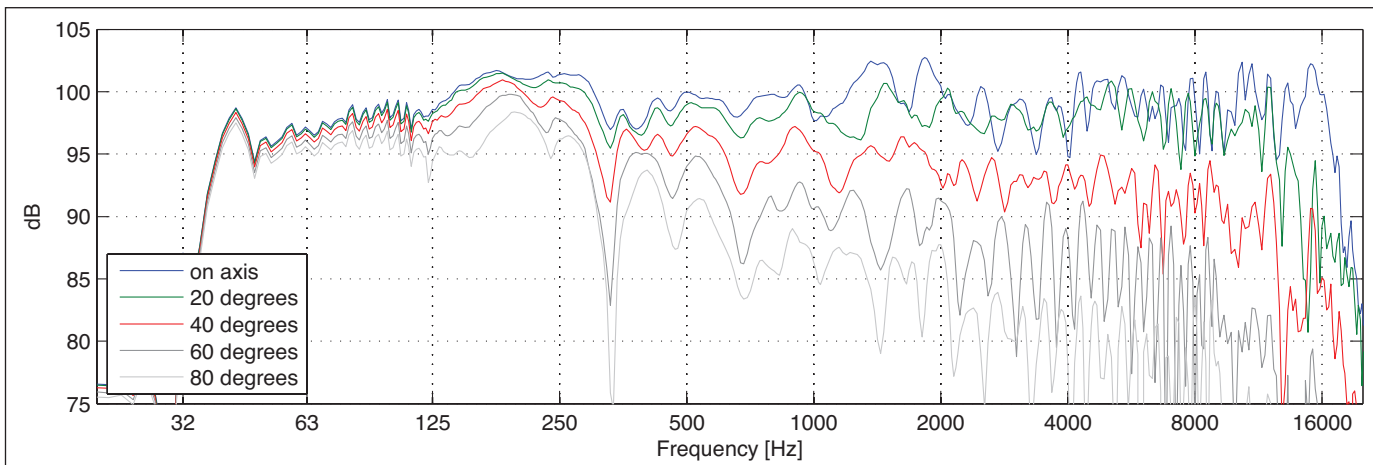


Figure 17. Responses at different angles with the loudspeaker 300mm (12 in.) from a woven screen.

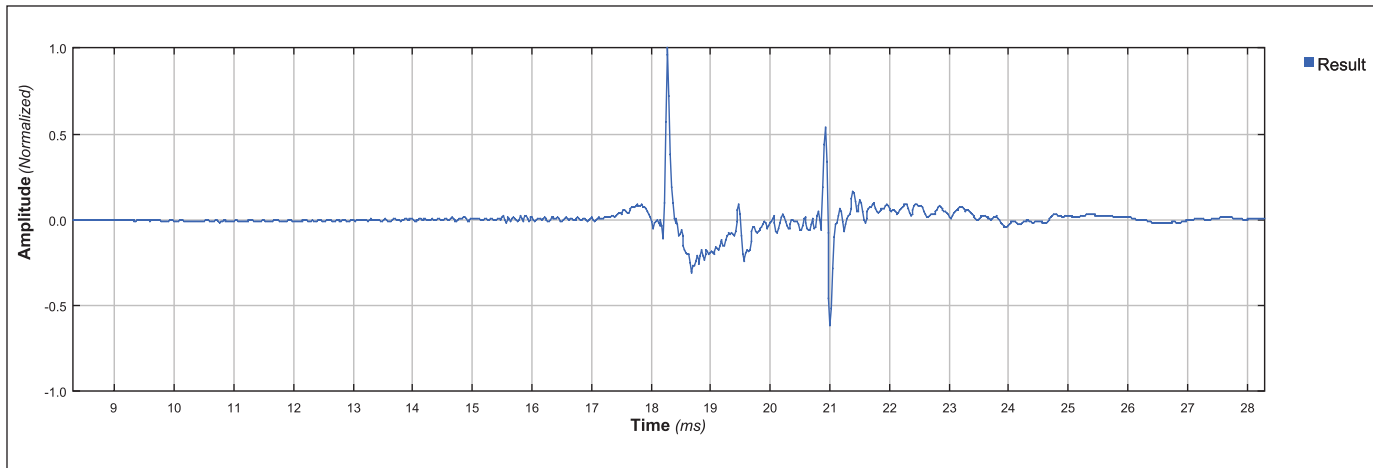


Figure 18. IR 60° off the horizontal loudspeaker axis with a mini-perf screen 300mm (12 in.) from the loudspeaker.

As the measurement points move farther off axis, the magnitude of the comb filtering increases, indicating that the direct and the reflected energies from behind the screen are more similar in level. This outcome is clearly visible in **Fig. 18**, which shows the IR measured 60° off the horizontal loudspeaker axis with mini-perf screen.

In **Figs. 19-21**, the effect of the screen-to-loudspeaker distance is examined at the on-axis measurement position, with the screen placed 150, 300, and 450mm from the loudspeaker. As the distance between the screen and the loudspeaker increases, the change to the frequency response becomes greater at lower frequencies. This effect appears to have a lower limit around 500 Hz for the perforated screens but continues to lower frequencies with the woven screen.

Figures 22-24 show the effect of the screen's distance to the speaker with a measurement point on the edge of the loudspeaker's specified coverage. These results show that as the distance between the loudspeaker and the screen increases, less comb filtering occurs in the off-axis responses.

PLANE WAVE TUBE MEASUREMENTS

Overview

Measurements of the normal-incidence acoustic properties of the three screen types were made using an aluminum plane wave tube and single microphone. This type of plane wave tube was first described by Stevens and Vanderkooy.⁷ Use of the tube to measure acoustic absorption coefficients is described by Leembruggen and Gilfillan.⁸

The method provides some worthwhile benefits over impedance tubes utilizing two microphones that are generally used today:

- Significantly reduced measurement times compared to the traditional two position methods
- A considerably smaller volume of data to be acquired
- Requirements of only single-channel instrumentation and one microphone
- Excellent high-frequency accuracy due to the elimination of mismatches in amplitude and phase between the two microphones



FURTHER INVESTIGATIONS INTO THE INTERACTIONS BETWEEN CINEMA LOUDSPEAKERS AND SCREENS continued

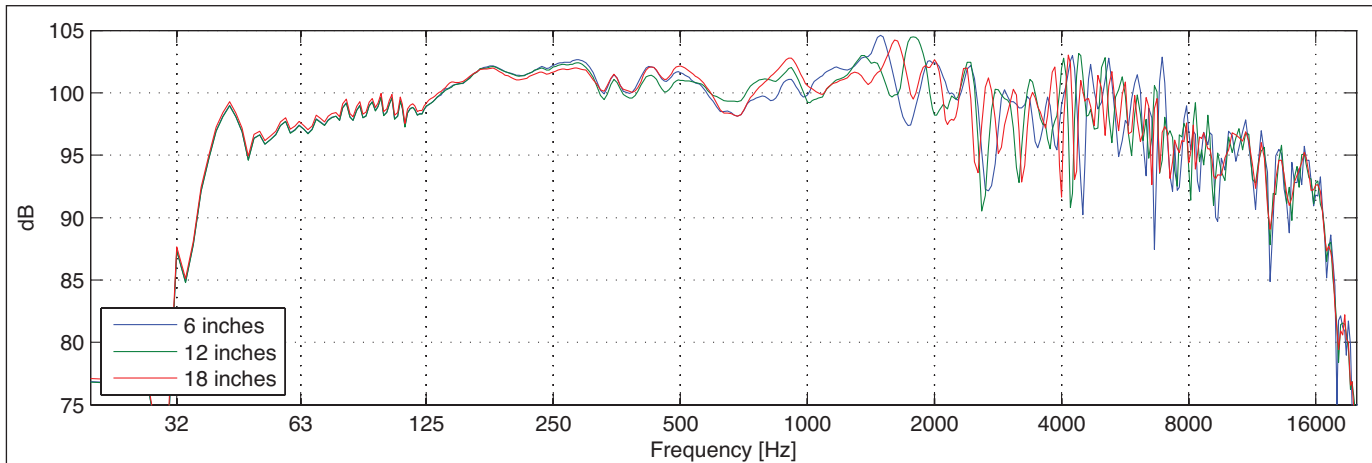


Figure 19. Effect of the distance of the loudspeaker from a theater-perf screen on axis at 150, 300, and 450mm (6, 12, and 18 in., respectively).

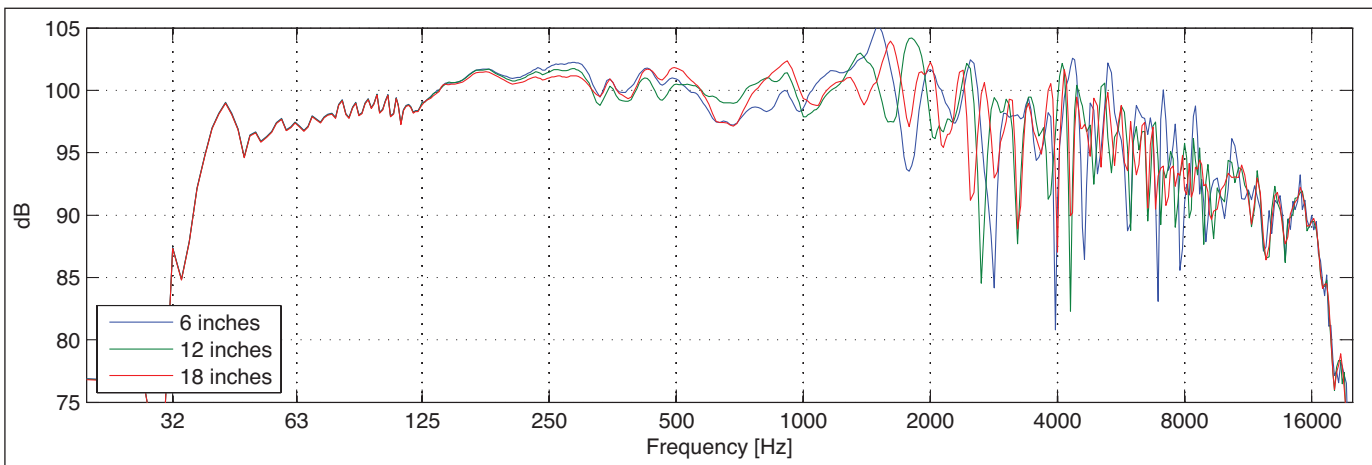


Figure 20. Effect of the distance of the loudspeaker from a mini-perf screen on axis at 150, 300, and 450mm (6, 12, and 18 in., respectively).

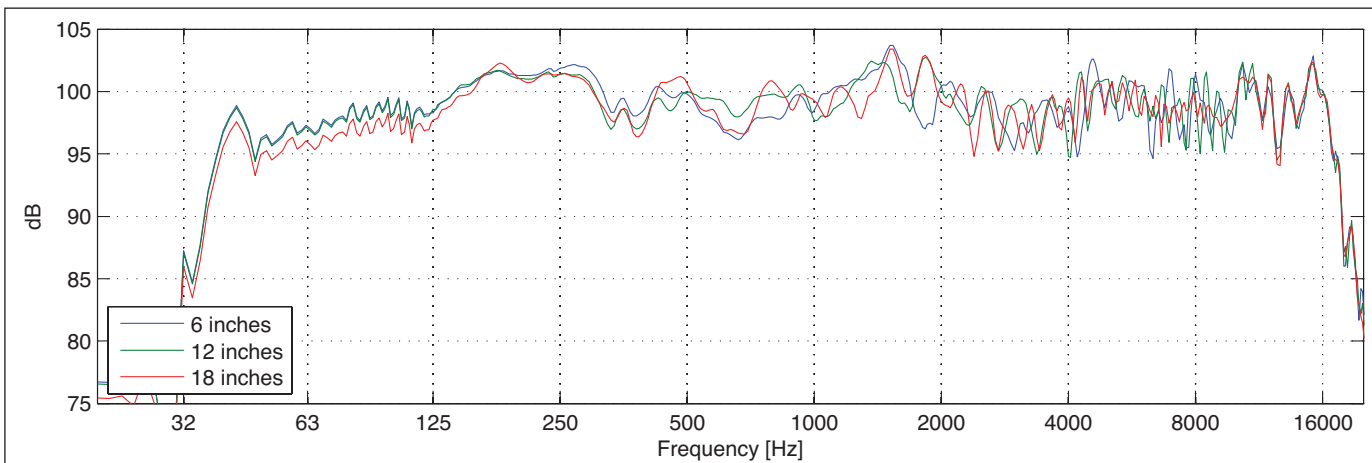


Figure 21. Effect of the distance of the loudspeaker from a woven screen on axis at 150, 300, and 450mm (6, 12, and 18 in., respectively).

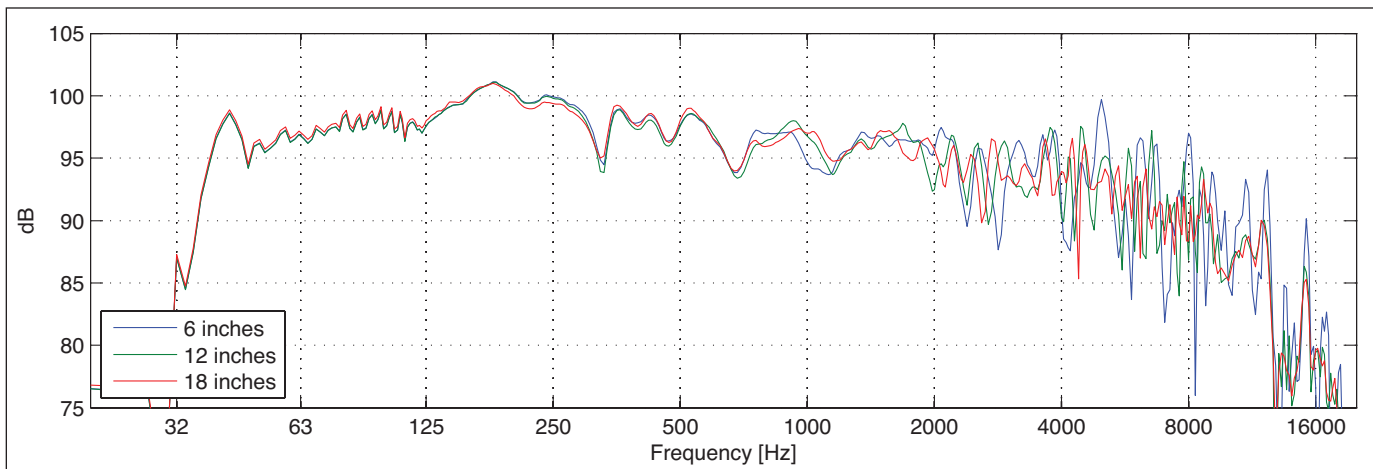


Figure 22. Effect of the distance of the loudspeaker from a theater-perf screen 40° off axis with the screen positioned at 150, 300, and 450mm (6, 12, and 18 in., respectively).

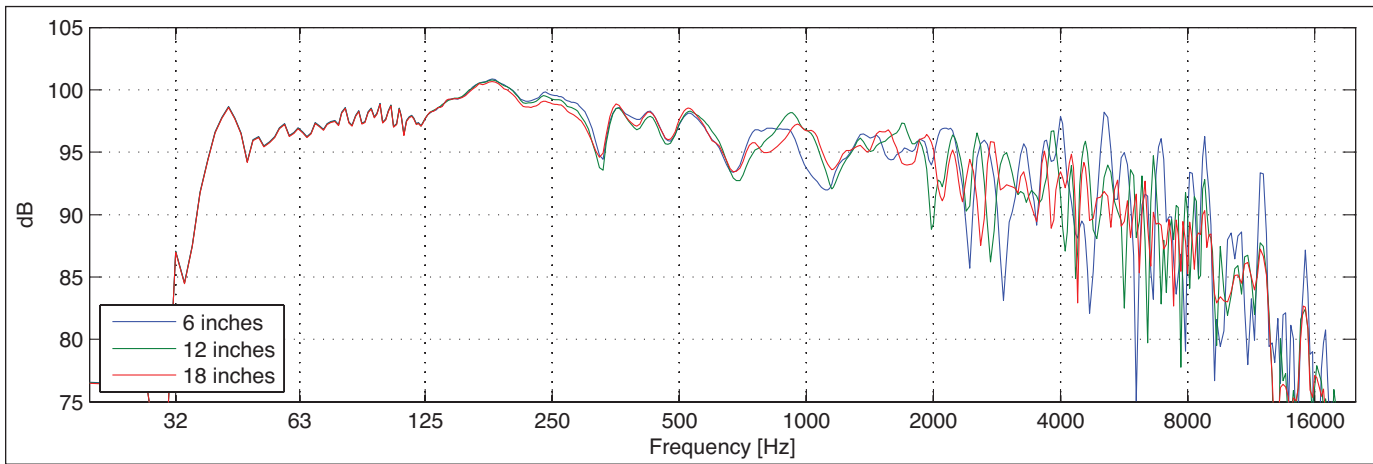


Figure 23. Effect of the distance of the loudspeaker from a mini-perf screen 40° off axis with the screen positioned at 150, 300, and 450mm (6, 12, and 18 in., respectively).

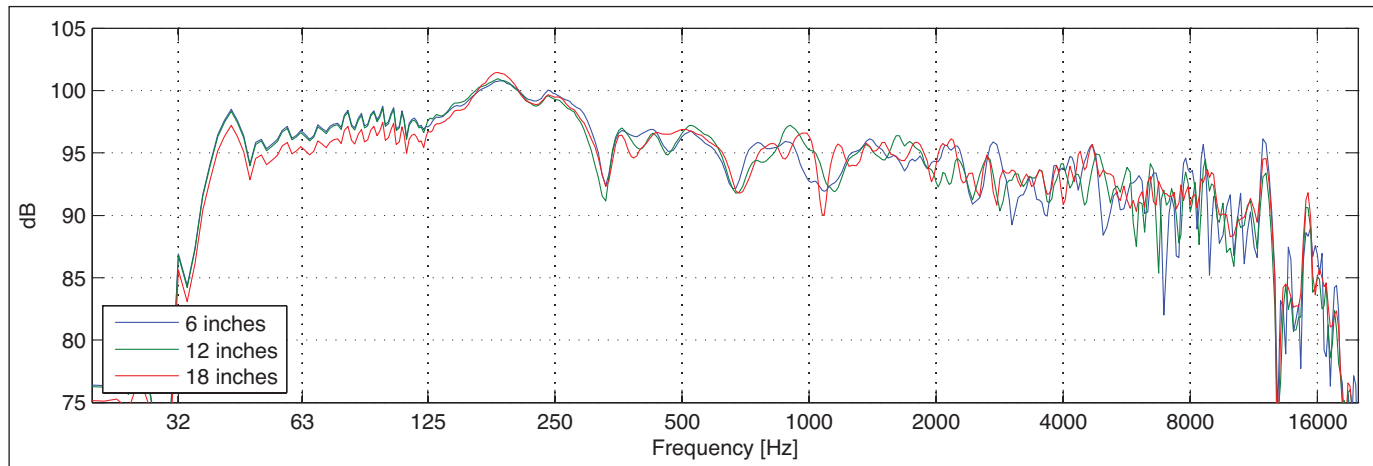


Figure 24. Effect of the distance of the loudspeaker from a woven screen 40° off axis with screen positioned at 150, 300, and 450mm (6, 12, and 18 in., respectively).

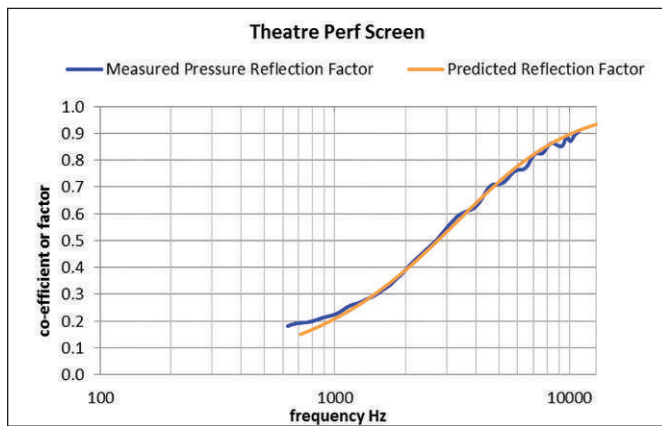


Figure 25. Measured and predicted behaviors of the theater-perf screen.

Knowledge of the normal-incidence reflection properties enables computation of the following acoustic parameters for each screen type:

- Pressure reflection factors (PRFs) both magnitude and phase
- Pressure transmission factors (PTFs); both magnitude and phase

The PRF at each frequency is the ratio of the reflected sound pressure to the incident sound pressure. The PRF ranges between 0 and 1, with 0 indicating a completely nonreflective surface and 1 indicating a value of a completely reflective surface.

The sound pressure transmitted through the screen, or PTF, cannot be computed from the reflection factor alone and was therefore measured directly. The PTF is the ratio of the transmitted sound pressure to the incident sound pressure and ranges between 0 and 1, with 0 indicating an acoustically opaque screen and 1 indicating a completely acoustically transparent screen.

Tube Setup

The appendix provides details about the setup of the tube, its acoustic response, and the process of calibration.

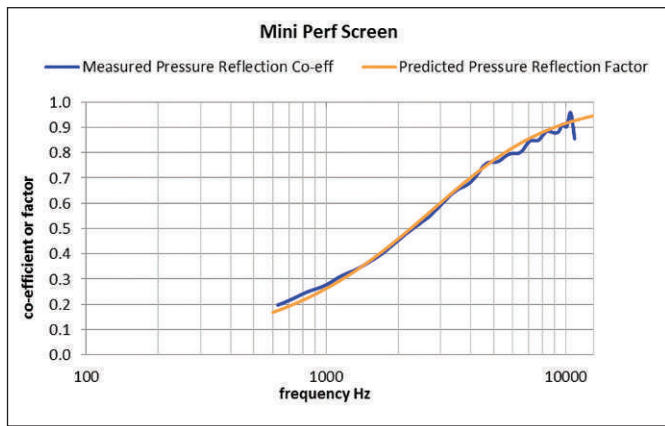


Figure 26. Measured and predicted behaviors of the mini-perf screen.

Prediction of Screen Properties

A method to compute the acoustic properties of a combination of layers of different materials is outlined by Colam and Leembruggen.⁹ Guy provides a good description of this method and shows how a system of many different layers can be modeled from knowledge of the individual layers' impedances and propagation constants and the continuity relationships between the layers.¹⁰ Cox and D'Antonio also describe this method, which they term the "transfer matrix method."¹¹

The computational model starts from a known terminating impedance and works through the multilayer system, calculating the transmission of sound through each layer according to the characteristic impedance and propagation constant of that layer. Layers consist of air, porous (foam or fibrous) and resistive material, limp masses, or perforated panels. A plane wave is assumed to be normally incident to the system. Equations of continuity are used at the junctions between individual layers. Equations given by Lee and Swenson¹² and by Maa¹³ for the acoustic impedance of the perforated screens are included in the model.

User inputs are the surface density of each mass, perforation ratio, hole diameter and material thickness of each perforated panel, and

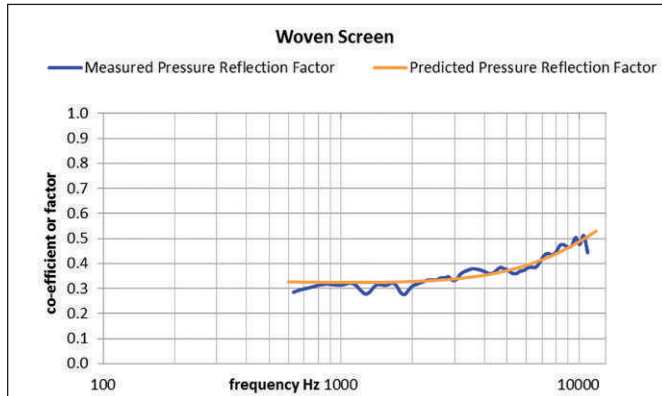


Figure 27. Measured and predicted behaviors of the woven fabric screen. The predicted results have been curve-fitted from estimated mass and resistance parameters.

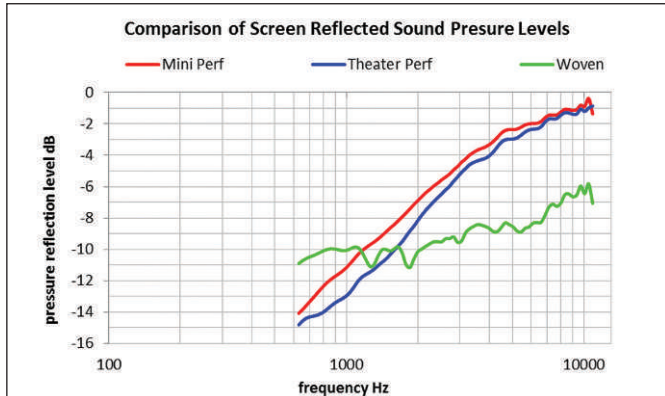


Figure 28. Reflected SPLs relative to incident sound levels for the three types of screen.

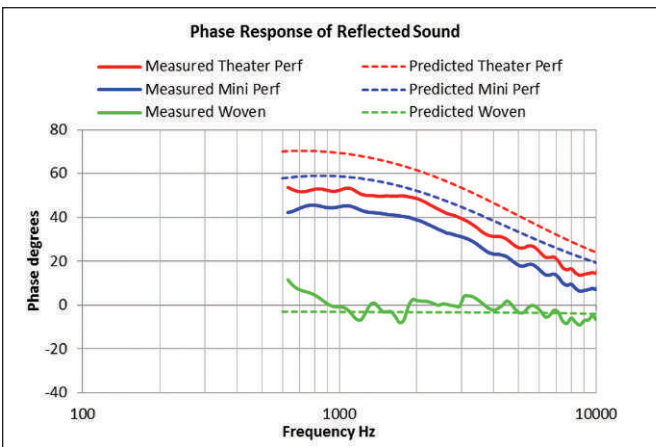


Figure 29. Phase responses of the reflected sound relative to the incident sound.

flow resistivity and thickness of the foam or fibrous materials and air gap distances.

Comparison of the measured and predicted absorption properties was undertaken by examining the sensitivity of the predicted absorption to small variations in the hole size, screen thickness, and perforation ratio. Because the number of holes exposed to the tube varies slightly according to the relative positions of the screen and tube, the effective perforation ratio in the tube can be slightly different from the nominal perforation ratio.

Results

Theater-Perf Screen

The measured and predicted behaviors of the theater-perf screen are compared in **Fig. 25**. Predictions were based on the measured material thickness (0.3mm), nominal hole size (1.2mm), and 13 holes visually exposed to the tube, producing an effective perforation ratio of 5.2% (cf. 4.5% nominal).

Figure 26 compares the measured and predicted behaviors of the mini-perf screen. Predictions were based on the measured material thickness (0.26mm), measured hole size (approximately 0.55mm),

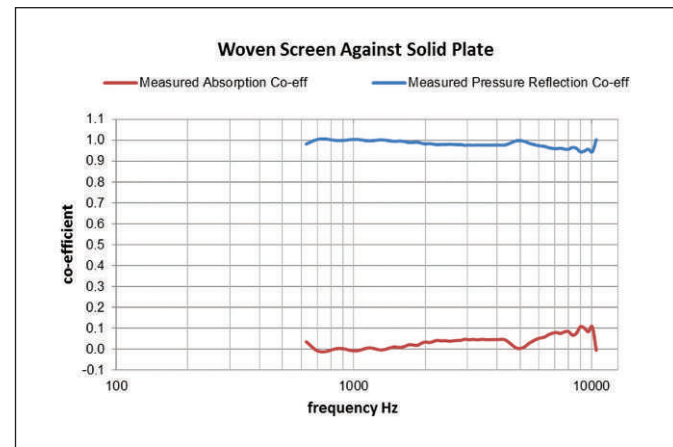


Figure 30. Measured absorption coefficients and reflection factors for the woven screen, which is located against a solid plate.

and 27 holes visually exposed to the tube, producing an effective perforation ratio of 2.66% (cf. 1.7% nominal).

Figure 27 compares the measured and predicted behaviors of the woven fabric screen. The frequency-dependent nature of the results suggests either a frequency-dependent loss or an effective moving mass component. Using a resistance value of 380 Rayls and a moving mass value of 8.2 g/m², our predictions show a good match to the measured data. We measured the actual flow resistance of the screen in our laboratory at 295 Rayls and measured, unexpectedly, the physical mass of the screen at 165 g/m², which is vastly different from the apparent moving mass of 8.2 g/m².

Reflected Sound Pressure Results

Converting the PRFs for the three screen types into logarithmic levels yields the results in **Fig. 28**, which are relative to a level of 0 dB from the loudspeaker arriving at normal incidence onto the screen.

The levels that are reflected back to the loudspeaker are remarkably high and indicate the need for acoustic absorption on the loudspeaker baffles and all local surfaces so that these reflections do not cause problems. Unless these reflections are absorbed, their subse-

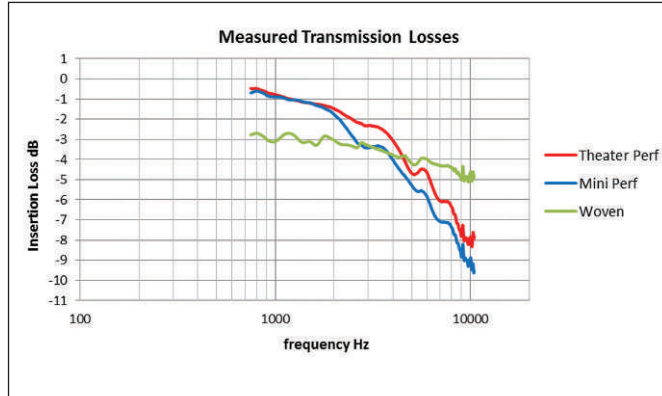


Figure 31. TL of each screen type.

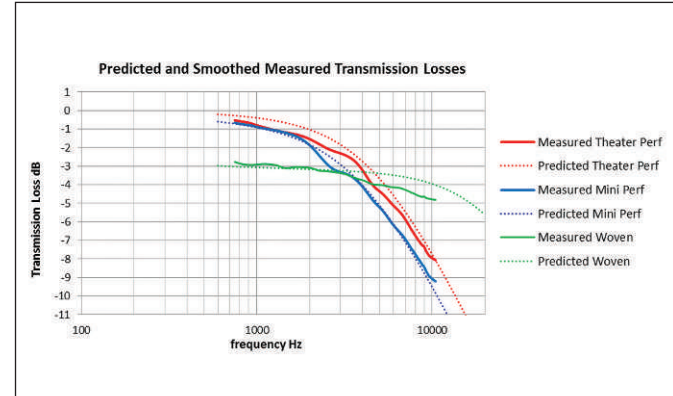


Figure 32. Comparison of predicted and smoothed measured TLs.



Frequency	TL Decibels (0.5-Octave Bandwidth)		
	Theater Perf	Mini Perf	Fabric
1 kHz	-0.8	-0.9	-2.9
3 kHz	-2.3	-3.3	-3.4
6 kHz	-5.1	-6.2	-4.1
10 kHz	-8.0	-9.1	-4.8

Table 1. Averaged TLs of screen types at specific frequencies.

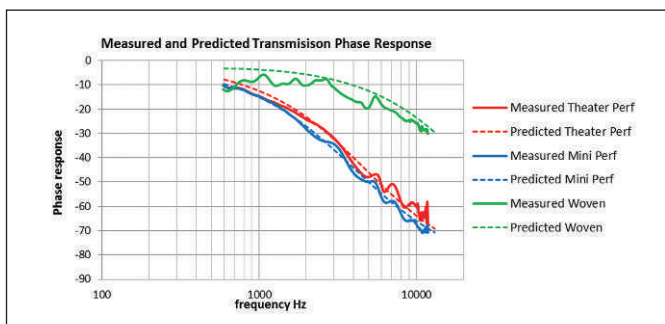


Figure 33. Comparison of measured and predicted phase responses of the three screen types.

quent reflections from loudspeakers or structures would result in degradation in frequency response and unwanted acoustic reflections from behind the screen.

At 10 kHz, with its “absorption” coefficient (which is calculated as $1 - \text{PRF}^2$) of 0.2, the perforated screens reflect as much sound power as a coarse, unpainted concrete block. In these terms, it is hard to imagine aiming a loudspeaker toward such a wall.

Reflected Phase Response Results

The phase responses of the reflected sound relative to the incident sound are shown in **Fig. 29** for the three screen types. Both measured and predicted responses are given for comparison.

With each of the measured responses, small delays of 70, 30, and 15 μsec were removed from the measured phase responses of the theater-perf, mini-perf, and woven screens, respectively, to bring them closer into agreement with the predicted responses. These delays most likely correspond to the differences in the starting times of the Fast Fourier Transform (FFT) window between the incident and the reflected pulses (see **Fig. 37** in the appendix for an illustration).

Actual Absorption of Woven Screen

To measure the actual absorption of the woven screen, the fabric was clamped directly in front of a solid endcap (**Fig. 36**). In this situation, the measured absorption coefficients can be directly related to the absorption of surface finishes, such as a carpet.

Figure 30 shows the measured absorption coefficients and reflection factors for the woven screen and indicates that little sound is absorbed by the fibrous material in the woven screen.

This measurement was not undertaken for the perforated screens, because they have essentially zero loss in this test situation:

- The screens contain no fibrous material to produce acoustic loss.
- When located against a solid boundary, the holes that in normal operation provide a combination of acoustic mass and resistance transform into short tubes that appear as an acoustic compliance.

Transmission Factor of Screens

The transmission factor of each screen type was assessed by measuring the pressure insertion loss with the screen located between the loudspeaker and the measurement microphone. The insertion loss is simply the difference between the received sound pressure levels (SPLs) with and without the screen in place. **Figure 31** shows the PTF or transmission loss (TL) in decibels.

Some minor measurement artifacts are evident, especially around 5 kHz, but the trends are clear.

To aid consideration of the relative TLs and compare the measured with the predicted data, the data of **Fig. 31** were smoothed over a bandwidth of 0.5 octaves. **Fig. 32** compares the smoothed-measured and predicted losses. (For the woven fabric screen prediction, the curve-fitted parameters were used.) The predictions of losses are close to the measured values.

To assist consideration of the results, **Table 1** enumerates the screen losses of **Fig. 32** at specific frequencies.

Transmission Phase Response of Screens

The transmission phase of each screen type was assessed by computing the difference in the phase responses at the microphone with and without the screen in place. The phase responses were

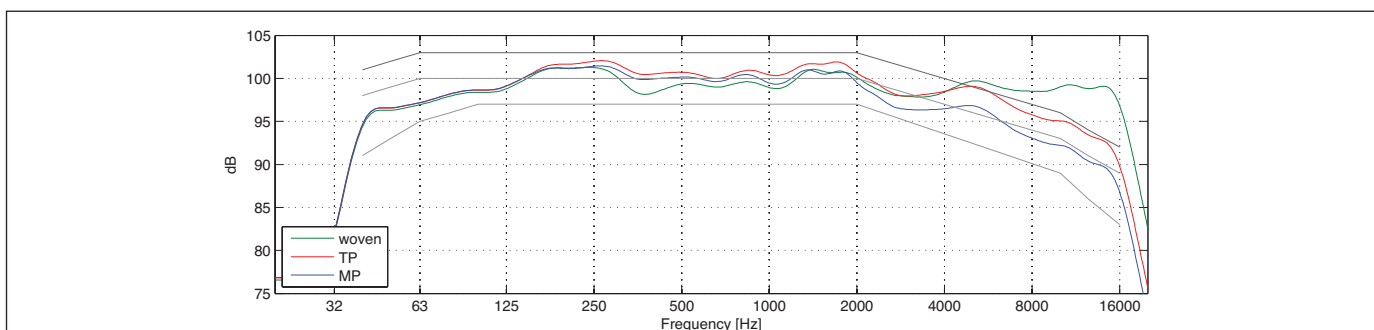


Figure 34. Third-octave smoothed on-axis response compared with the X curve.

also predicted. Small delays of 55, 59, and 110 μ sec were removed from the measured phase responses of the theater-perf, mini-perf, and woven screens, respectively, to bring them into agreement with the predicted responses. These delays most likely correspond to the difference in the starting times of the FFT window between the no-screen and the with-screen cases.

Figure 33 compares the measured and predicted phase responses of the three screen types.

The phase responses of the perforated screens are similar and show agreement within 10° with the predicted phase responses. The agreement between the measured and the predicted for the woven screen is also within 10° , based on the curve-matched parameters discussed earlier.

CONCLUSION

Measurements of the interaction between loudspeaker and cinema screen have been conducted in an anechoic chamber. In addition, measurements of the screen reflection and transmission properties have been conducted in a plane-wave tube. Both series of measurements have confirmed that the perforated screens reflect a substantial amount of sound energy at higher frequencies and that the woven screen is more acoustically transparent.

Analysis of the impulse and frequency response data for the loudspeaker-screen system shows that the interaction of screen and loudspeaker is complex and that interference between direct and reflected sound causes substantial changes in the loudspeaker's radiation pattern and frequency responses due to comb filtering.

The reflections from the perforated screens are particularly strong at high frequencies and directly related to the effective acoustic mass of the screen material and perforations. At 10 kHz, the perforated screens reflect as much sound energy as a coarse-grained, unpainted concrete block.

The energy that is reflected back to the loudspeaker is subsequently reflected back to the screen with only a minor reduction in level and arrives sufficiently soon after the direct sound to cause complex comb filtering.

The reflection and transmission properties of the woven screens can be primarily modeled by a simple acoustic resistance. Although lower than their perforated counterparts, both these properties are sufficiently high to warrant consideration in the design of cinema systems.

The high-resolution time and frequency domain measurements used in this study did not reveal the occurrence of a beam-spreading Fresnel lens effect. Instead, they showed that the increased levels beyond the loudspeaker's coverage pattern are due to complex interference between the reflected pressure and the weaker direct field pressure (resulting from being a long way off axis). When these responses are smoothed, the interference effects are masked and the beam appears to have spread. However, the roughness of the responses in this area compromises the listening experience. The measurements in earlier referenced studies did not show the telltale signs of reflections in the IRs or comb filtering in the frequency responses.

Increasing the distance between the loudspeaker and the screen reduces the frequency at which the on-axis frequency responses are affected by complex interference between direct and reflected sound; however, increasing this distance reduces the overall severity of the peaks and troughs in the responses within the specified coverage pattern.

With the perforated screens, the on-axis loss of the transmitted level above 5000 Hz is relatively severe, and restoring the frequency responses requires significant equalization. With the high crest factors at high frequencies of soundtracks and the equalization required for high-frequency, constant-directivity horns, the additional equalization for screen losses greatly increases the demands on the available output voltages of the electronics. With the fabric screen, the average

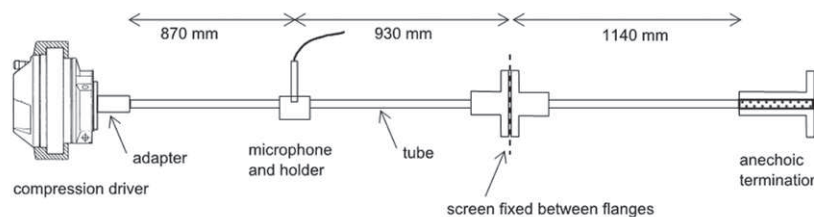


Figure 35. Arrangement of the plane-wave tube to measure screen reflection and absorption properties.

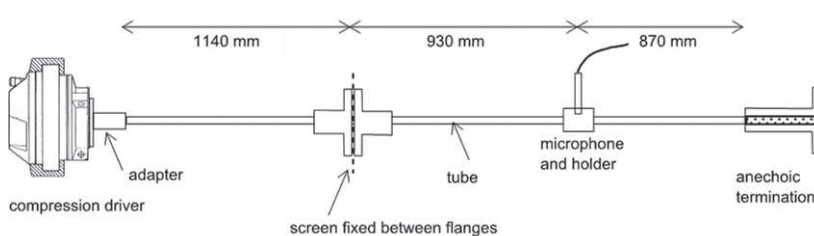


Figure 36. Arrangement of the plane-wave tube to measure screen TL properties.

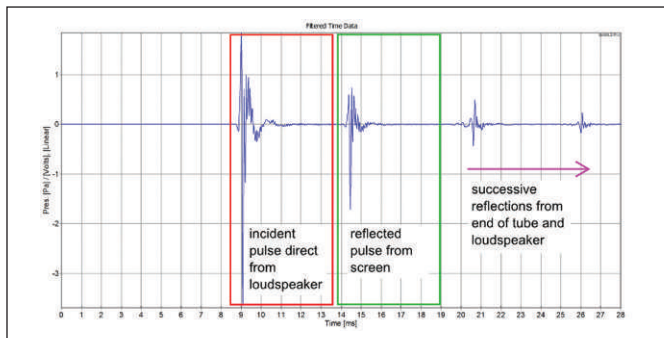


Figure 37. Example of an IR at the microphone.

loss is approximately 3 dB, and accommodating this loss requires doubling of all amplifier power compared to the no-screen situation.

Because the comb filtering effects are different at different angles, no single equalization can properly correct the overall spatial response. Equalization could actually exacerbate the effects of the reflected sound.

The sound reflected by the screen can also be directed away from the loudspeaker and into the acoustical space behind the screen. Depending on the acoustical absorption in that space, this reflected energy (1) could eventually travel back through the screen to listeners and (2) would, if it arrives sufficiently early after the direct field, further degrade the frequency responses over the listening area.

As shown in **Fig. 34**, when the on-axis frequency response is smoothed over a third octave bandwidth, the loudspeaker's frequency response falls in the tolerance bands of the SMPTE 202:2010 X-curve standard when the theater-perf and mini-perf screens are used. We conclude that the screen itself is one of the greatest contributors to the frequency response observed in a cinema. In contrast, the woven screen shows a much flatter response.

Magnitude and phase responses of the pressure reflection and transmission factors for each screen type with normal sound incidence have been presented.

The degree to which perforated screens actually absorb the sound is negligible. In the case of the woven screen, the absorption is negligible up to 2 kHz and minimal at higher frequencies.

Based on the strong agreement of the measured and the predicted behaviors of the screens in the plane-wave tube, we conclude that the theoretical acoustic models of screens are well documented, and in this context, it is surprising that their impact on cinema sound has not been properly addressed to date.

APPENDIX

The plane-wave tube consists of two sections of aluminum tube with a 19 mm internal diameter and 3 mm wall thickness. A JBL 2426H 25 mm (1 in.) compression driver is connected to one end of the first tube via a tapered adapter and produces sound in the tube over the frequency range of 600 Hz to 15 kHz.

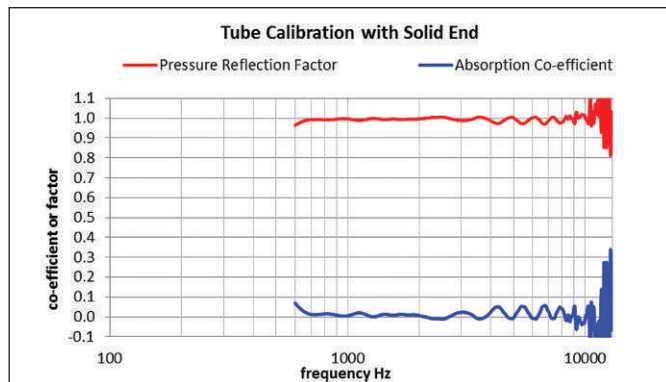


Figure 38. Corrected absorption and reflection parameters in the tube with a solid endcap.

The two lengths of tube are joined by two back-to-back flanges, between which the screen sample under test is clamped. Oversize holes were punched in the screen samples to ensure that the screens were free of the threads of the screws used to clamp the flanges together.

Figure 35 shows the conceptual arrangement of the plane-wave tube for measuring the reflection and absorption properties, while **Fig. 36** shows the arrangement for measuring the transmission properties.

The 1140 mm long section of the tube downstream of the screen sample provides a pseudoanechoic environment for the screen for a brief period before reflections from the end of the tube arrive. Although not essential for the tube operation, high-performance polyester sound insulation (Martini Industries PolyMax XHD50) was fitted into a 200mm long holder screwed onto the end of the second tube to provide a virtually anechoic termination. The packing density of the insulation was graded, with the end nearest the screen being loosely packed.

The loudspeaker is driven with a swept-sine wave signal, produced by WinMLS 2004 acoustic analyzer software. The resulting sound in the tube is picked up by a 12.5 mm Type 1 microphone, and its output is processed by the WinMLS 2004 analyzer. The microphone's signal is mathematically deconvolved with the swept-sine wave signal to produce the IR of the tube system at the microphone.

The distances between driver, microphone, screen sample, and end section are sufficiently large to allow the incident pulse and the subsequent reflected pulses to be reasonably separated in time so that (1) the decaying tail of the incident pulse does not intrude into the start of the reflected pulse and (2) the decaying tail of the reflected pulse from the screen does not intrude into the start of the subsequent reflected pulses.

The 19mm diameter of the tube imposes an upper frequency limit to the tube operation of approximately 10.4 kHz. At this frequency, the first transverse mode in the tube appears, at which point plane-wave behavior ceases. At particular frequencies above 10.4 kHz, sound waves cease to propagate along the tube and exist as circular standing waves across the tube.

Parametric, high and low pass filtering was used to

- Limit the low-frequency response of the loudspeaker to above 600 Hz

- Flatten the frequency response of the direct-field sound pressure as a visual aid
- Remove frequencies above 10.4 kHz so that they did not dominate the IR and cause spectral leakage when the IRs were truncated by the rectangular windows

Acoustic Response of the Tube

The IR of the system consists of a number of pulses that progressively decay over time, of which an example is given in **Fig. 37**. The following pulses, in time order, are clearly visible:

- The forward-traveling (or incident sound wave), which has traveled directly along the tube from the loudspeaker; this pulse is ultimately incident on the screen material
- The backward-traveling wave (toward the loudspeaker), which is the reflection of the incident from the screen material
- A succession of pulses, which result from successive forward- and backward-traveling reflections of sound from:
 - The loudspeaker phase plug
 - The screen under test
 - The end of the tube

The time response is truncated or “windowed” using a rectangular window to separate the incident sound from the reflected sound.

Using the FFT, the frequency contents of the incident and reflected waves were computed from the windowed time data. The ratio of the magnitude of the reflected sound to the incident sound was then found at each frequency, which provided the complex PRFs as follows:

$$r = P_- / P_+ \quad (1)$$

where r is the PRF, P_+ is the complex incident pressure reaching the microphone direct from the loudspeaker, and P_- is the complex reflected pressure reaching the microphone direct from the sample.

From the magnitude of the PRF at each frequency, sound absorption coefficient A is computed as follows:

$$A = 1 - r^2 \quad (2)$$

The complex (real and imaginary) components of the acoustic impedance Z of the absorption material at each frequency can be also computed from the complex pressure reflection coefficients at each frequency:

$$Z = \frac{1 + r}{1 - r} \quad (3)$$

Calibration of Tube Losses

Losses in the tube (aside from reflection from the sample under test) are due to viscothermal effects in the tube and increase with frequency. The combination of Eq. 4 from Stevens and Vanderkooy⁷ and Eq. 5 from Chu¹⁴ gives the predicted tube loss as a function of frequency:

$$\tau_{\text{tube-test}} = e^{-\frac{\alpha L}{c}} \quad (4)$$

with

$$\alpha = 0.0204 \sqrt{f / cD} \quad (5)$$

where α is the loss factor, L is the length of the tube in meters, f is the frequency in hertz, c is the speed of sound in meters per second, and D is the diameter of the tube in meters.

The tube system was calibrated by fixing a solid endcap onto the tube and comparing the frequency responses of the incident and first-reflected pulses. With a solid endcap on the tube, the reflection factor should be unity, and the absorption coefficient should be zero.

The losses predicted by Eq. 4 were found to be higher than those measured, and by curve fitting, an alternative constant term of 0.0105 for α in Eq. 5 was found for our system.

Using the reciprocal of Eq. 4, the primary tube losses associated with the reflected pulse were removed. The resulting pressure reflection and absorption coefficients are shown in **Fig. 38**. The large spikes in the responses above 10 kHz indicate the presence of the cross-modes in the tube.

The remaining ripples in the responses result from tiny errors of up to 0.15 dB in the reflected pulse, and these secondary errors were removed by a simple inverse correction. Both the primary and the secondary correction factors were applied to all reflected spectra in the measurements presented.

REFERENCES

1. J. Eargle, J. Bonner, and D. Ross, “The Academy’s New State-of-the-Art Loudspeaker System,” *SMPTE J.*, 94:667–675, 1985.
2. J. Allen, J. Hunter, K. Geist, and R. Delgado, “Employing Specific Loudspeaker Designs Which Can Substantially Reduce Motion Picture Screen Interference and Losses,” presented at the 132nd SMPTE Technical Conference, New York, NY, Oct. 1990.
3. J. Baird and P. Meyer, “The Analysis, Interaction, and Measurement of Loudspeaker Far-Field Polar Patterns,” presented at the 106th Audio Engineering Society Convention, Munich, preprint 4949, May 1999.
4. J. Meyer, P. Meyer, and J. Baird, “Far-Field Loudspeaker Interaction: Accuracy in Theory and Practice,” presented at the 110th Audio Engineering Society Convention, Amsterdam, preprint 5309, May 2001.
5. F. Seidel and H. Staffeldt, “Frequency and Angular Resolution for Measuring, Presenting and Predicting Loudspeaker Polar Data,” *J. Audio Eng. Soc.*, 44(7/8), July/Aug. 1996. M. Barron, *Auditorium Acoustics*, Spon Press, 2003.
6. Meyer Sound Laboratories, MAPP Online Pro Cinema, <http://www.meyersound.com/products/mapponline/cinema/register/>.
7. R. Stevens and J. Vanderkooy, “A Novel Single-Microphone Method of Measuring Acoustical Impedance in a Tube,” presented at the 115th AES Convention, paper 5901, 2000.
8. G. Leembruggen and D. Gilfillan, “Comparison of Measured and Predicted Sound Absorption Properties of Polyester Fibre Insulation Using an Unusual Plane Wave Tube,” *Proc. I/OA ’10*, presented at Reproduced Sound Conference, UK 2010.



9. S. Colam and G. Leembruggen, "Analysis and Design of Acoustic Absorbers and Low Frequency Transmission Loss," *Proc. IOA '03*, presented at Reproduced Sound Conference, UK 2003.
10. R. Guy, "A Preliminary Study Model for the Absorption or Transmission of Sound in Multi-Layer Systems," *Noise Contr. Eng. J.*, 33(3), Nov. 1989.
11. T. Cox and P. D'Antonio, *Acoustic Absorbers and Diffusers: Theory, Design, and Application*, Spon Press: New York, NY, 2004.
12. J. Lee and G. Swenson, "Compact Sound Absorbers for Low Frequencies," *Noise Contr. Eng. J.*, 38(3):109-117, 1992.
13. D. Y. Maa, "Potential of Microperforated Panel Absorber," *J. Acoust. Soc. Am.*, 104(5):2861-2866, Nov. 1998.
14. W. Chu, "Extension of the Two-Microphone Transfer Function Method for Impedance Tube Measurements," *J. Acoust. Soc. Am.*, 80:1, 1986.

BIBLIOGRAPHY

- Eargle, J.; Mayfield, M.; and Gray, David, "Improvements in Motion Picture Sound: The Academy's New Three-Way Loudspeaker System," *SMPTE J.*, 106:464-476, 1997.
- M. Rettinger, "Sound Transmission Through Perforated Screens," *SMPTE J.*, 91:1171-1174, 1982.
- Schultz, T., *Acoustical Uses for Perforated Materials: Principles and Applications*, Industrial Perforators Association: Milwaukee, WI, 1986.
- Seidel, F., and Staffeldt, H., "AES Information Document for Room Acoustics and Sound Reinforcement Systems—Loudspeaker Modeling and Measurement—Frequency and Angular Resolution for Measuring, Presenting, and Predicting Loudspeaker Polar Data" (AES-5id-1997), *J. Audio Eng. Soc.*, 46(3):195-216, 1998.

Presented at the SMPTE 2012 Annual Technical Conference & Exhibition, 23-25 October 2012. Copyright © 2012 by SMPTE.

THE AUTHORS



Brian Long has more than 15 years in professional audio and a diverse and extensive knowledge regarding the design and implementation of sound reinforcement and playback systems for all types of scenarios ranging from simple single speaker events to massive show spectacles and multichannel media presentation environments. Long holds a Master of Fine Arts from the University of Southern California's School of Cinematic Arts, where he specialized in post-production audio and worked on advanced multichannel audio concepts. He is currently a member of the engineering team at Skywalker Sound.



Glenn Leembruggen is a principal of the consulting engineering firms of Acoustic Directions and ICE Design in Australia and is also an Associate of Sydney University. Playing saxophone in a Chicago style electric blues band, Leembruggen is quite passionate about the left and right brain aspects of sound (physics and the aural experience) and his work designing rooms and sound systems to deliver extremely high quality speech and music. His current work is with courts, parliaments, transport terminals, road tunnels and cathedrals. Among Leembruggen's research interests are the differences that exist between subjective and measured speech intelligibility, cinema sound and the measurement and prediction of acoustic absorption. He is member of the Audio Engineering Society (AES), ASA, IOA, and SMPTE and is part of the Maintenance Team for the STI standard IEC 60268-16.



Roger Schwenke, PhD, is a senior scientist and has been contributing his expertise in acoustic measurement and prediction at Meyer Sound Laboratories for over ten years. Schwenke's expertise in acoustics has been applied towards making acoustical measurements and recommendations, including the design and tuning Constellation systems, at world class venues around the world. He has participated in the development of a number of the company's innovative products, including MAPP Online, SIM 3, Constellation Electroacoustic Architecture, the M1D UltraCompact Curvilinear Array Loudspeaker, and LD-3 Compensating Line Driver. Schwenke received a Doctorate in Acoustics from Penn State University in December of 2000; his thesis work in advanced detection and estimation methods was sponsored by the Applied Research Laboratory. He is a member of the Acoustical Society of America.



Peter Soper has been a member of Meyer Sound's Technical staff since 1986. He holds several design and technical patents for loudspeaker technology, and is a member of SMPTE and the Audio Engineering Society.